Nano Energy (2014) **10**, 192–200

Available online at www.sciencedirect.com

ScienceDirect

journal homepage: www.elsevier.com/locate/nanoenergy

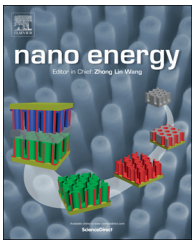

RAPID COMMUNICATION

Electrospun porous nanorod perovskite oxide/nitrogen-doped graphene composite as a bi-functional catalyst for metal air batteries

Hey Woong Park[a], Dong Un Lee[a], Pouyan Zamani[a], Min Ho Seo[a], Linda F. Nazar[b,*], Zhongwei Chen[a,*]

[a]*Department of Chemical Engineering, Waterloo Institute for Nanotechnology, Waterloo Institute for Sustainable Energy, University of Waterloo, Waterloo, Ontario, Canada N2L 3G1*
[b]*Department of Chemistry, Waterloo Institute for Nanotechnology, University of Waterloo, Waterloo, Ontario, Canada N2L 3G1*

KEYWORDS
Perovskite oxide;
Graphene;
Metal-air batteries;
Bi-functional catalysts;
Durability

Abstract
The current generation is not only facing the shortage of fossil fuels in the near future, but also is responsible for preserving the environment for future generations. As a result, the development of clean energy systems is becoming an urgent focus for the research community. Metal air batteries have attracted much attention due to their extremely high energy density, and the rechargeability which is directly governed by the oxygen reduction reaction (ORR) and oxygen evolution reaction (OER). Herein, we present a new class of hybrid bi-functional catalyst consisting of porous nanorod perovskite $La_{0.5}Sr_{0.5}Co_{0.8}Fe_{0.2}O_3$ (LSCF-PR) combined with nitrogen-doped reduced graphene oxide (NRGO) active towards both ORR and OER. The novel morphology of LSCF-PR is prepared by an electrospinning method, and incorporated into NRGO sheets. Electron microscopy reveals interesting composite morphology in which LSCF-PR is embedded between the sheets of NRGO, forming an efficient LSCF-PR/NRGO composite morphology for the electrochemical oxygen reactions. Electrochemical testing of the LSCF-PR/NRGO composite in alkaline medium results in excellent ORR and OER catalytic activities, verifying the effective combination for bi-functionality. LSCF-PR/NRGO presents not only a comparable or superior performance to state-of-the-art Pt/C catalyst for ORR or OER, respectively, but also better durability. These results highlight the applicability of LSCF-PR/NRGO composite having unique and efficient morphology as a promising bi-functional catalyst for metal air battery applications.

*Corresponding authors.
E-mail addresses: lfnazar@uwaterloo.ca (L.F. Nazar), zhwchen@uwaterloo.ca (Z. Chen).

http://dx.doi.org/10.1016/j.nanoen.2014.09.009
2211-2855/

Introduction

Metal air batteries based on lithium, zinc, aluminum, etc. have been introduced in the literature as a primary battery using oxygen (O_2) from atmospheric air to generate energy [1,2]. However, recent efforts have been focused on the development of the rechargeable battery systems, and improving their practical energy densities. To make this possible, however, highly efficient bi-functional catalysts active towards both the oxygen evolution reaction (OER) and oxygen reduction reaction (ORR) are required to lower the large overpotentials associated with charging and discharging the rechargeable metal air battery, respectively [3,4]. To date, carbon supported precious metals such as platinum (Pt)-based materials or iridium (Ir)-based materials have been considered as the best ORR or OER catalysts, respectively [5,6]. However, the high prices of these precious metals and the limited bi-functional activity to catalyze both the oxygen reactions on a single electrode have hampered the realization of wide commercialization. To address this, much effort has been put into developing effective and cost-effective bi-functional catalysts such as carbon nanotube or grapheme-supported transition metal oxides, which shows excellent ORR and OER activities [7,8]. Especially, graphene has played a significant role for energy conversion systems [9,10], including support of catalysts owing to its unique structure and high electrical conductivity [11]. In fact, it has been reported that heteroatom-doped graphene by boron (B), nitrogen (N) or sulfur (S) generates electrocatalytic active sites, especially for ORR in alkaline medium [12-14]. Perovskite oxides have also received much attention as efficient electrode materials due to its relatively high electronic and ionic conductivity [15-18]. Shao-Horn and co-workers reported the trends in ORR and OER activities of perovskite oxides, introducing underlying design principles for perovskite based electrocatalysts [19-21]. Additionally, they highlighted the importance of large surface areas on perovskite catalyst activity, particularly towards the OER [22]. Drawing on this, Xu et al. [23] have proposed porous $La_{0.75}Sr_{0.25}MnO_3$ nanotubes by electrospinning, focusing on the catalytic activities in organic electrolytes, while Zhao et al. [24] have produced mesoporous perovskite $La_{0.5}Sr_{0.5}CoO_{2.91}$ nanowires by a multistep microemulsion method. Nevertheless, further improvements to the oxygen catalysis are still necessary in order to utilize them as practical bi-functional catalysts.

Here, we introduce uniquely structured composite materials consisting of porous $La_{0.5}Sr_{0.5}Co_{0.8}Fe_{0.2}O_3$ nanorods (LSCF-PR) and nitrogen-doped reduced graphene oxide (NRGO). This nanostructured LSCF-PR/NRGO composite characterized physicochemically and electrochemically presents as a new class of bi-functional catalyst for rechargeable metal-air batteries. Particularly, the facile electrospinning method produces homogeneous nano-structured perovskite materials with unique porous nanorod morphology. NRGO prepared using a thermal annealing method in the presence of NH_3 is then incorporated with LSCF-PR for providing ORR activity and simultaneously acting as a conductive support [25]. For the first time, these nanomaterials are coupled into a novel hybrid design to produce bi-functional catalyst with excellent activities towards both the ORR and OER, with superior durability, rendering LSCF-PR/NRGO as a highly promising electrode material for the next generation rechargeable metal-air battery systems.

Experimental section

Synthesis of LSCF-PR catalyst.

Perovskite oxide of LSCF-PR was prepared by the electrospinning method with metal precursors and polymer solution. The solution was prepared by completely dissolving La$(NO_3)_3 \cdot 6H_2O$, Sr$(NO_3)_2$, Co$(NO_3)_2 \cdot 6H_2O$ and Fe$(NO_3)_3 \cdot 9H_2O$ in H_2O, C_2H_5OH and DMF with 2:5:4 mass ratio along with 15.4 wt% PVP. The solution was electrospun at a distance of 15 cm between the needle tip of syringe and a ground Al foil collector with an applied voltage of 23 kV using home-made D.C. power supply. The injection rate was controlled to 0.5 mL min^{-1} by a syringe pump (New Era Pump System Inc. Model no. NE-300). The electrospun fibers were dried at 60 °C in an oven overnight and collected. To obtain perovskite oxide of LSCF-PR, the collected fibers were calcined at 700 °C for 3hr in air. As control materials, LSCF-NP was prepared using the same electrospinning solution, and LCO-NP was prepared by only using La$(NO_3)_3 \cdot 6H_2O$ and Co$(NO_3)_2 \cdot 6H_2O$ dissolved in the same solvent as LSCF-PR. Both of these solutions were directly calcined using the same condition of 700 °C for 3 h with a heating rate of 1 °C min^{-1} as LSCF-PR.

Synthesis of NRGO

For NRGO preparation in this study a one-step exfoliation and nitrogen doping method using graphene oxide (GO) prepared by a modified Hummer's method was applied as we reported elsewhere [25]. First, a 100 mg of GO was loaded at the end of a long quartz tube and the quartz tube was placed in a horizontal tube furnace with GO placed outside the heating zone. Once the temperature in the furnace reached to 1100 °C the quartz with 50 sccm of Ar/NH_3 mixture gas flow was moved until GO shifted to the heating zone. After 10 min, the tube was returned to its initial position and allowed to cool in order to obtain NRGO. For un-doped RGO, only Ar gas was utilized but it was prepared using the same process.

Preparation of LSCF-PR/NRGO composite and electrochemical characterization

LSCF-PR/NRGO composite was prepared by dispersion in 0.3 wt% nafion/ethanol solution. 30 wt% LSCF-PR and 70 wt. % NRGO were mixed in the Nafion solution with total concentration of 4 $mg_{catalyst}$ ml^{-1}. The solution was sonicated for 3 h until no precipitation was shown. To examine electro-catalytic activities, the solution was coated onto a glassy carbon rotating disk electrode (RDE) with catalyst loading of 0.41 mg cm^{-2}. As control catalysts, NRGO, Pt/C or Ir/C catalyst electrode was prepared in the same way. To investigate electro-catalytic activity of LSCF-PR itself, LSCF-PR and LSCF-NP electrode were prepared in the same way with catalyst loading of 0.20 mg cm^{-2}. A platinum (Pt) wire and saturated calomel electrode (SCE) were utilized as

counter and reference electrode, respectively. Linear sweep voltammetry (LSV) and cyclic voltammetry (CV) were conducted with a potentiostat (CH Instrument, Electrochemical Workstation) and were used to investigate electro-catalytic activities in N_2 or O_2-saturated 0.1 M KOH at a scan rate of 10 mV s^{-1} at a rotation speed of 900 rpm controlled by a rotation speed controller (Pine Instrument Co., AFMSRCE). The LSV for ORR activity was conducted in the potential range of 0.1 V to −1.0 V (vs. SCE) by cathodic scan in N_2 and O_2-saturated 0.1 M KOH, while the CV for OER activity was conducted in the potential range of 0–1.0 V (vs. SCE) in O_2-saturated 0.1 M KOH commencing with the anodic scan. For the ORR polarization curve, the double-layer charge effect was removed by subtracting the polarization curve obtained in N_2-saturated 0.1 M KOH. The OER polarization curve was shown with average response of anodic and cathodic scan in this work. Note that ORR and OER polarization curves were displayed in a single graph to clearly show the catalyst's bi-functional ORR and OER activities. For further analysis of ORR activity, various rotation speeds such as 100 rpm, 400 rpm, 900 rpm and 1600 rpm were applied during LSV. All potentials displayed in this work were converted from vs. SCE to vs. reversible hydrogen electrode (RHE), based on the conversion equation, $E_{RHE}=E_{SCE}+0.241\ V+0.059\times$ pH, with the pH of 0.1 M KOH being 13 [26]. In addition, the chronoamperometry (CA) technique was applied to assess the durability during ORR and OER in O_2- and N_2-saturated 0.1 M KOH electrolyte, respectively. −0.4 V (vs. SCE) for ORR and 0.8 V (vs. SCE) for OER were applied and current retention versus operating time was plotted to show the catalysts' durability.

Material characterization

Scanning electron microscopy (SEM) (LEO FESEM 1530) and transmission electron microscopy (TEM) (Philips CM300) were used to observe the morphology and structure of the developed catalysts. High-resolution and TEM (HRTEM) and selected area electron diffraction (SAED) were utilized to investigate the crystallinity. X-ray diffraction (XRD) (AXS D8 Advance, Bruker) was conducted to confirm crystal structures. X-ray photoelectron spectroscopy (XPS) (K-Alpha XPS spectrometer, Thermal Scientific) was used to analyze chemical elements and chemical configuration.

Results and discussion

Figure 1 illustrates the preparation of LSCF-PR/NRGO hybrid, whereby polyvinylpyrrolidone (PVP)-metal based fibers are obtained by electrospinning and then subjected to a calcining heat treatment at 700 °C for 3 h in air to decompose PVP and obtain crystalline LSCF-PR. NRGO is prepared via rapid annealing of graphite oxide (GO) under Ar/NH_3 gas flow. After the preparations of LSCF-PR and NRGO, the two materials are mixed in ethanol-diluted Nafion solution by sonication to finally obtain LSCF-PR/NRGO hybrid bi-functional catalysts. Figure 2(a) presents SEM image of the electrospun fibers before calcination of LSCF-PR, which confirms the electrospinning conditions produces bead- and aggregate-free homogeneous fibers. Upon calcination however, the morphology of the fibers changes to a uniform rod shape, as shown in Figure 2(b) and (c). During calcination, PVP is decomposed and the metal precursors stabilize into the unique porous nanorod structure. The TEM image in Figure 2(d) further highlights the nanorods having the porous rod morphology, with clearly observable pores on the surface highlighted by the white arrows. Elemental analysis of LSCF-PR by energy-dispersive X-ray spectroscopy (EDS) presents the distribution of the atoms as shown in the color map in Figure 2(e). The EDS element images verify that all elements in LSCF are detected and well-dispersed throughout the porous nanorod structure. To determine the crystalline structure of the synthesized LSCF-PR, the X-ray diffraction (XRD) pattern (Figure 2(f)) was analyzed and found to be characteristic of a single phase crystalline perovskite oxide with a rhombohedrally distorted structure and space group R-3c, consistent with previous reports having the same chemical composition [16,24,27,28]. This is further evidenced by the select area electron diffraction (SAED) pattern (Figure 2(d) inset) and high resolution TEM (HR-TEM) image

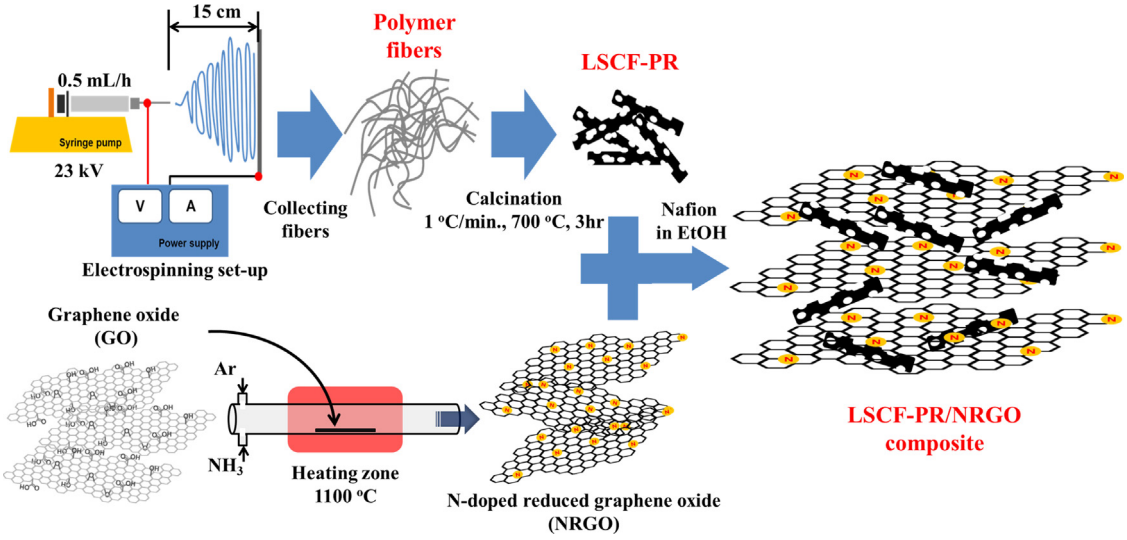

Figure 1 Schematic illustration of the preparation of LSCF-PR/NRGO composite.

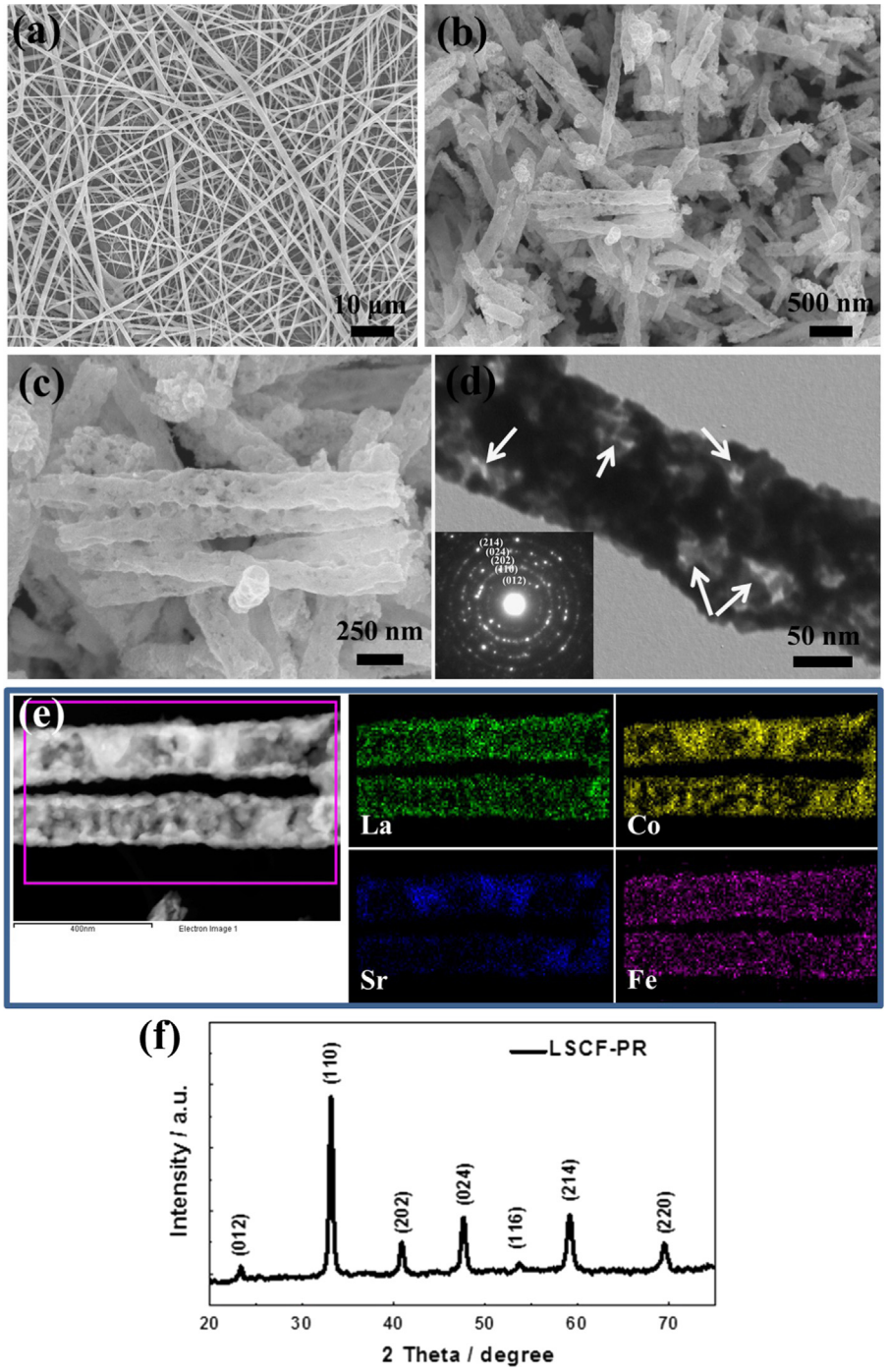

Figure 2 SEM images of (a) electrospun fibers containing metal precursors and PVP, (b,c) LSCF-PR after calcination of the fibers; (d) TEM image of LSCF-PR (inset: SAED pattern); (e) elemental mapping by EDS from TEM; and (f) XRD pattern of LSCF-PR.

(Figure S1). The *d*-spacing measured by the observed fringes in the HR-TEM image are 0.270 and 0.229 nm, consistent with the theoretical *d*-spacing of the (110) and (202) planes of LSCF perovskite oxide, respectively.

As an effective substrate for good distribution of LSCF-PR and excellent ORR catalyst [8,29], NRGO is synthesized via a facile heat treatment which makes it highly active towards the ORR [25]. SEM and TEM images present a two-dimensional voile-like architecture of graphene sheets which effectively provides electron conductive pathways in an electrode (Figure 3(a) and (b)). Un-doped RGO is also prepared by the same method except in absence of NH_3 as a comparison. Distinguishing between RGO and NRGO based on electron microscope characterization is difficult [30], hence X-ray photoelectron spectroscopy (XPS) has been conducted and confirmed nitrogen content and its configurations within the graphitic layer of NRGO sheets, compared with RGO (Figure S2) [31]. To investigate the electrode structure of LSCF-PR/NRGO

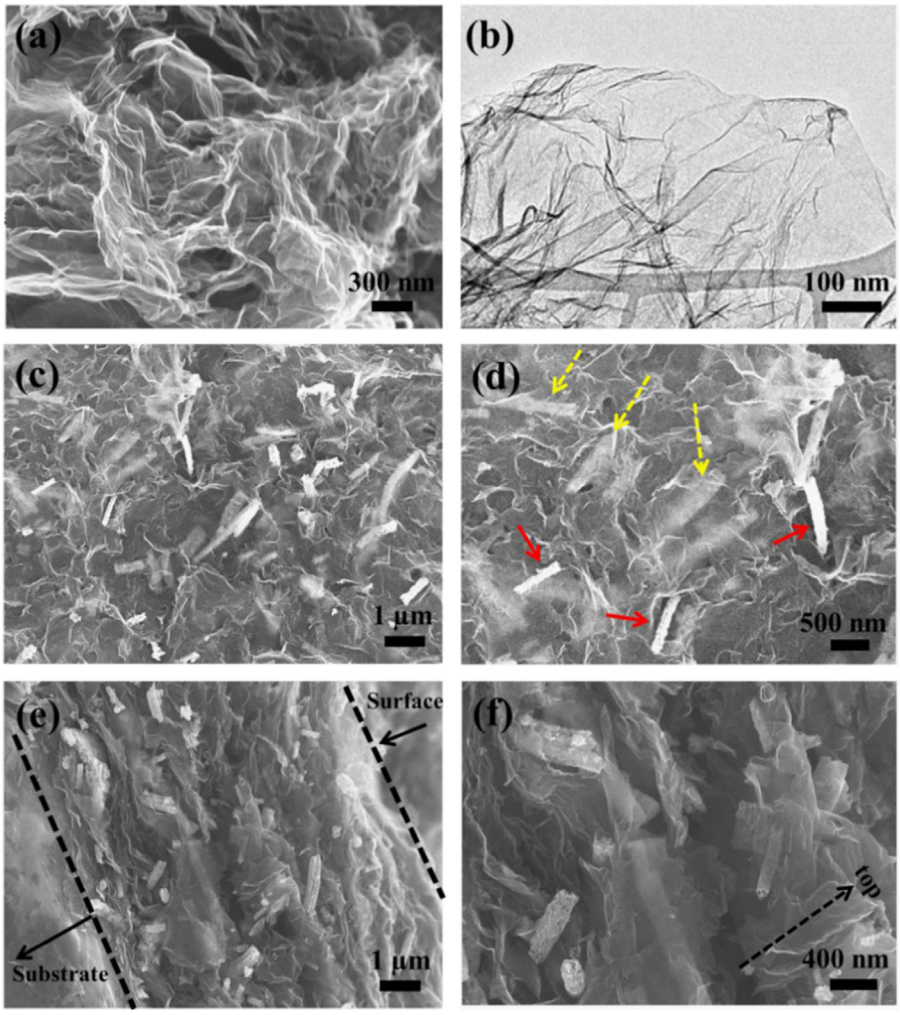

Figure 3 SEM and TEM images of (a,b) NRGO; SEM images of (c,d) LSCF-PR/NRGO composite; and cross-sectional SEM images of the (e,f) LSCF-PR/NRGO composite.

composite prepared by mixing in the Nafion solution, the composite are coated on an aluminum foil by the same procedure as the preparation of the working electrode for all electrochemical testing. The SEM image in Figure 3 (c) shows LSCF-PR well-dispersed throughout the sheets of NRGO. Moreover, a magnified image in Figure 3(d) clearly shows some LSCF-PR buried under the graphene sheets (dotted arrows) and others exposed on the surface (solid arrows). The cross-sectional SEM image of LSCF-PR/NRGO electrode is also provided in Figure 3(e) showing a three-dimensional structure with well-distributed LSCF-PR throughout the sheets of NRGO. The magnified cross-section image shows consistent morphologies observed with in-plane of the composite with both buried and exposed LSCF-PR incorporated in the graphene sheets (Figure 3(f)). It is believed that this novel structure of the composite catalyst is attributed to the amphiphilic property of Nafion effectively combines hydrophobic NRGO with relatively hydrophilic LSCF-PR since the Nafion ionomer has been known to be a good surfactant for dispersing carbon-based structures such as CNT and graphene due to its amphiphilic property [32,33]. Additionally, LSCF nanoparticles (LSCF-NP) and $LaCoO_3$ nanoparticles (LCO-NP) have also been synthesized as comparisons to compare the morphological and compositional effects. The morphology and crystal phase of LSCF-NP and LCO-NP is also characterized by SEM and TEM, and XRD (Figures S3 and S4, respectively). While these materials demonstrate the same crystal structures, LSCF-NP exhibits irregularly shaped nano-sized particles with some aggregation. The specific surface area, pore size distribution and pore volume of LSCF-PR and LSCF-NP are analyzed by nitrogen adsorption and desorption isotherms at 77 K using the Brunauer–Emmett–Teller (BET) and Barrett–Joyner–Halenda (BJH) methods (Figure S5). The BET surface area and BJH total pore volume of LSCF-PR is 36.5 $m^2\,g^{-1}$ and 0.139 $cm^3\,g^{-1}$, respectively, which has much larger surface areas compared to the respective values of LSCF-NP (22.6 $m^2\,g^{-1}$ and 0.113 $cm^3\,g^{-1}$), owing to the nanorod morphology with high porosity as observed by the electron micrographs. This directly shows that electrospinning and subsequent calcination process are highly beneficial for the preparation of perovskite oxide based materials with significantly increased surface area.

The electrochemical behaviors of LSCF-PR, LSCF-NP and LCO-NP towards the ORR ($O_2+2H_2O+4e^-\rightarrow 4OH^-$) and OER ($4OH^-\rightarrow O_2+2H_2O+4e^-$) are investigated by half-cell

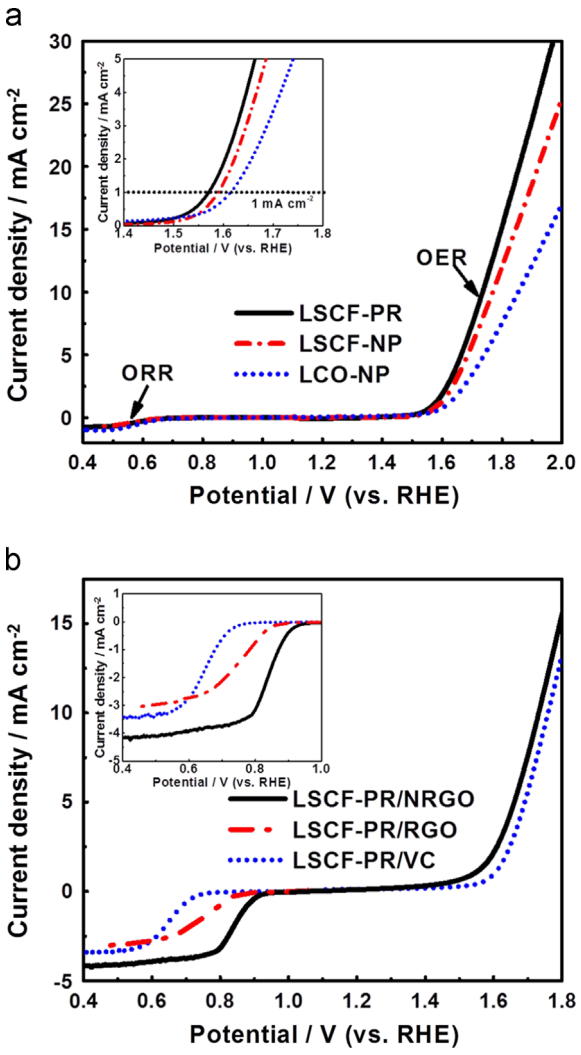

Figure 4 (a) ORR (negative scan) and OER (positive scan) polarization profiles at 900 rpm of LSCF-PR, LSCF-NP and LCO-NP (inset: magnified OER polarization profiles) and (b) ORR and OER polarization profiles at 900 rpm of LSCF-PR/NRGO, LSCF-PR/RGO and LSCF-PR/VC composites (inset: magnified ORR polarization profiles).

testing in 0.1 M KOH. Figure 4(a) displays full range polarization curves of ORR and OER of LSCF-PR and its comparison in O_2-saturated 0.1 M KOH between 0.4 V and 2.0 V (vs. RHE) scanned at 10 mV s^{-1}, showing cathodic and anodic currents associated with ORR and OER, respectively. While the metal oxides show relatively low current densities that are comparable to each other, clear differences are observed in OER activities with prominent current densities [7,34]. The OER potentials are measured at 1 mA cm^{-2}, the current density at which distinguishable electrochemical reaction kinetics occurs apart from the double-layer capacitance, where LSCF-PR shows much lower potential than those of LSCF-NP and LCO-NP (Figure 4(a) inset). The increased OER activity of LSCF-PR is also evidenced by significantly enhanced current densities observed at all electrode potentials investigated up to 2.0 V. The higher current densities and reduced overpotentials for OER of LSCF-PR compared to its nanoparticles counterpart are attributed to the porous nanorod morphology which provides larger surface areas significantly enhancing the active site exposure [20]. In addition, the porous structure also facilitates the diffusion of hydroxide ions during the electrocatalytic reaction which accelerates the kinetics of OER. With respect to the compositional advantages of LSCF-PR, the same perovskite phased LCO is significantly outperformed due to the Sr- and Fe-substitution which improve the catalytic activity towards the OER [16,35]. The effectiveness of combining LSCF-PR and NGRO as a bi-functional catalyst is shown in Figure 4(b), where the polarization profile of the composite shows far superior ORR behavior compared to RGO and Vulcan carbon (VC) composites, which is also confirmed by the cyclic voltammograms (Figure S6). Compared to LSCF-PR tested itself as shown in Figure 4(a), combining with a carbon support improves the ORR activity, while the OER activity remains similar to that of free LSCF-PR. In comparing ORR activities, half-wave potential of LSCF-PR/NRGO is 89 and 187 mV higher, and limiting current density at 0.4 V is increased by 1.08 and 0.76 mA cm^{-2} in comparison to LSCF-PR/RGO and LSCF-PR/VC composite, respectively (Figure 4(b) inset). This clearly highlights the benefits of using NRGO support, providing excellent ORR activity in alkaline conditions. Based on these results, the ORR and OER performance of LSCF-PR/NRGO is very similar to NRGO and LSCF-PR, respectively (Figure S7). This clearly confirms that the composite's ORR activity is mainly attributed to NRGO, while the OER activity is responsible for LSCF-PR, indicative of effective bi-functionality of the composite obtained by combining LSCF-PR and NRGO without interfering each other. In addition to the evaluation of the intrinsic ORR activity of LSCF-PR/NRGO catalyst, rotating disk electrode (RDE) measurements at various rotation speeds have been conducted to quantify the number of electrons transferred during the ORR. Based on the RDE measurements, Koutechý-Levich (K-L) plots have been prepared by selecting four different potentials of 0.75, 0.70 and 0.65 V as shown in Figure S8, demonstrating calculated *n* values of 3.9–4.0, and indicating that LSCF-PR/NRGO facilitates ORR by the highly efficient pseudo 4 electron pathway. Lastly, commercial Pt/C catalyst is examined to compare with LSCF-PR/NRGO catalyst as shown in Figure 5(a) and (b), which shows ORR performance of LSCF-PR/NRGO comparable to that of Pt/C in terms of limiting current density, and half-wave potential. In addition, the Tafel plot in the ORR potential region results in the slope of 60.0 mV/decade for LSCF-PR/NRGO which is similar to that of Pt/C (58.6 mV/decade) (Figure S9). To study the durability of LSCF-PR/NRGO catalyst, chronoamperometry is carried out at −0.4 V and 0.8 V (vs. SCE) for ORR and OER respectively, at rotation speed of 900 rpm to evaluate the reaction currents. As shown in Figure 5(c) and (d), the retention of current density of LSCF-PR/NRGO during ORR and OER is relatively stable compared to that of Pt/C, indicating superior durability of LSCF-PR/NRGO for bi-functional catalytic activity. Moreover, Ir/C catalyst as the state-of-the-art OER catalyst was examined for further investigation of the OER activity of LSCF-PR/NRGO composite. The OER polarization curves show that LSCF-PR/NRGO composite demonstrates slightly lower performance to that of the state-of-the-art Ir/C catalyst (Figure S10(a)). However, the differences in the

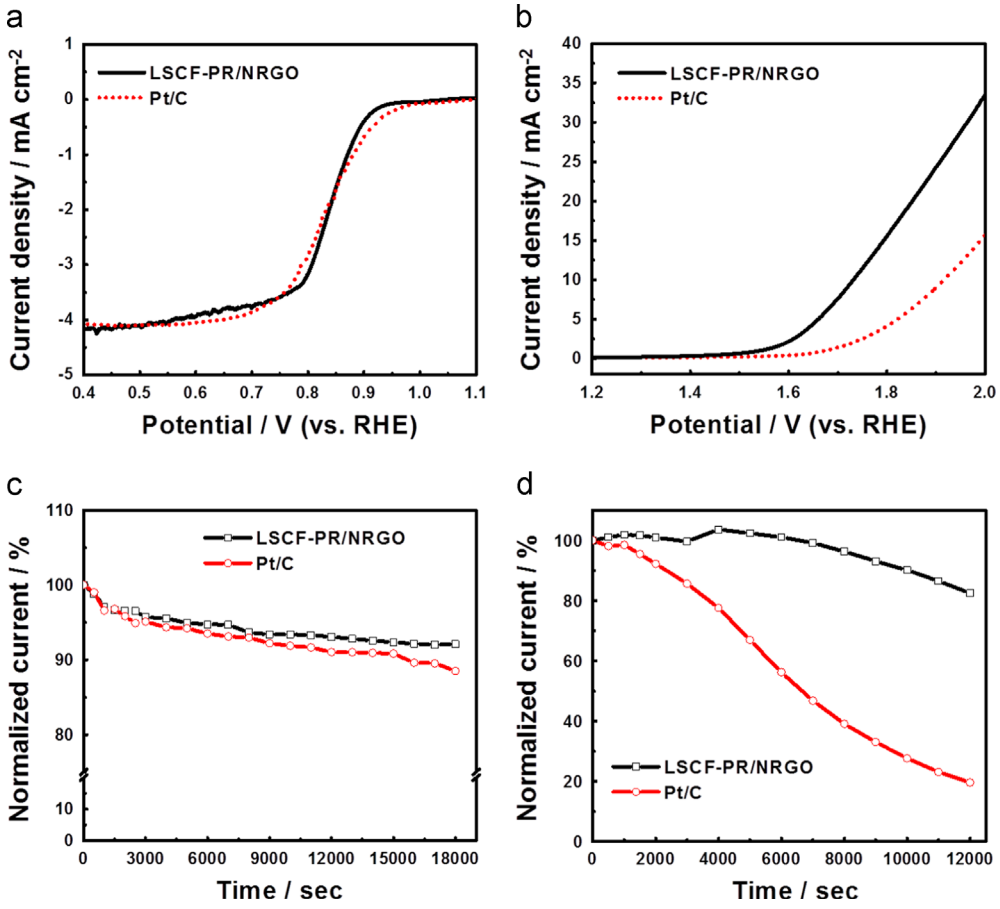

Figure 5 (a) ORR and (b) OER polarization profiles of LSCF-PR/NRGO and Pt/C; and chronoamperometric responses (percentage of current retained versus operation time) at 900 rpm for (c) ORR (−0.4 V vs. SCE) and (d) OER (0.8 V vs. SCE) of LSCF-PR/NRGO and Pt/C.

potential at 1 mA cm^{-2} and the current density at 2.0 V (vs. RHE) are only 30 mV and 5.7 mA cm^{-2}, respectively. In terms of OER durability, Ir/C catalyst presents inferior performance compared to LSCF/NRGO composite as demonstrated by the CA test (Figure S10(b)), similar to the premature degradation of the Pt/C catalyst. These results in combination with the ORR evaluation conducted with Pt/C catalyst testify that non-precious metal catalyst LSCF-PR/NRGO composite is capable of providing highly competitive bi-functional activities.

Conclusions

In conclusion, we introduce a technique to prepare perovskite oxide/nitrogen-doped graphene composites as highly active bi-functional catalysts for rechargeable metal-air battery applications. The novel porous nanorod morphology of LSCF-PR uniformly distributed throughout the NRGO sheets creates an efficient LSCF-PR/NRGO composite morphology for oxygen reactions. The electrochemical performances of the composite highlight excellent catalytic activity and better durability (compared to Pt/C) for both the ORR and OER in alkaline electrolytes. LSCF-PR is found to provide the majority of the OER activity, whereas NRGO provides the majority of the ORR active, resulting in a complementary bi-functional catalyst composite arrangement. Therefore, the uniquely designed composite LSCF-PR/NRGO catalyst with excellent electrochemical activity is highly promising for rechargeable metal-air batteries.

Acknowledgments

This research was supported by the Natural Sciences and Engineering Research Council of Canada (NSERC) through grant (no. 468306-2014) to Prof. Zhongwei Chen and the University of Waterloo.

Appendix A. Supplementary materials

Supplementary data associated with this article can be found in the online version at http://dx.doi.org/10.1016/j.nanoen.2014.09.009.

References

[1] J.S. Lee, S.T. Kim, R. Cao, N.S. Choi, M. Liu, K.T. Lee, J. Cho, Adv. Energy Mater. 1 (2011) 34–50.
[2] F.Y. Cheng, J. Chen, Chem. Soc. Rev. 41 (2012) 2172–2192.

[3] Z.L. Wang, D. Xu, J.J. Xu, X.B. Zhang, Chem. Soc. Rev. (2014). http://dx.doi.org/10.1039/c1033cs60248f.
[4] M. Prabu, K. Ketpang, S. Shanmugam, Nanoscale 6 (2014) 3173–3181.
[5] Y. Gorlin, T.F. Jaramillo, J. Am. Chem. Soc. 132 (2010) 13612–13614.
[6] Y. Lee, J. Suntivich, K.J. May, E.E. Perry, Y. Shao-Horn, J. Phys. Chem. Lett. 3 (2012) 399–404.
[7] Z. Chen, A.P. Yu, D. Higgins, H. Li, H.J. Wang, Z.W. Chen, Nano Lett. 12 (2012) 1946–1952.
[8] Y.Y. Liang, Y.G. Li, H.L. Wang, J.G. Zhou, J. Wang, T. Regier, H.J. Dai, Nat. Mater. 10 (2011) 780–786.
[9] Z.L. Wang, D. Xu, H.G. Wang, Z. Wu, X.B. Zhang, Acs Nano 7 (2013) 2422–2430.
[10] Z.S. Wu, G.M. Zhou, L.C. Yin, W. Ren, F. Li, H.M. Cheng, Nano Energy 1 (2012) 107–131.
[11] Z.L. Wang, D. Xu, J.J. Xu, L.L. Zhang, X.B. Zhang, Adv. Funct. Mater. 22 (2012) 3699–3705.
[12] S.B. Yang, L.J. Zhi, K. Tang, X.L. Feng, J. Maier, K. Mullen, Adv. Funct. Mater. 22 (2012) 3634–3640.
[13] Z.H. Sheng, H.L. Gao, W.J. Bao, F.B. Wang, X.H. Xia, J. Mater. Chem. 22 (2012) 390–395.
[14] D. Higgins, Z. Chen, D.U. Lee, Z.W. Chen, J. Mater. Chem. A 1 (2013) 2639–2645.
[15] W. Yang, J. Salim, S. Li, C. Sun, L. Chen, J.B. Goodenough, Y. Kim, J. Mater. Chem. 22 (2012) 18902–18907.
[16] E.M. Garcia, H.A. Taroco, T. Matencio, R.Z. Domingues, J.A.F. dos Santos, Int. J. Hydrog. Energy 37 (2012) 6400–6406.
[17] C. Jin, X.C. Cao, F.L. Lu, Z.R. Yang, R.Z. Yang, Int. J. Hydrog. Energy 38 (2013) 10389–10393.
[18] J. Sunarso, A.A.J. Torriero, W. Zhou, P.C. Howlett, M. Forsyth, J. Phys. Chem. C 116 (2012) 5827–5834.
[19] J. Suntivich, H.A. Gasteiger, N. Yabuuchi, H. Nakanishi, J.B. Goodenough, Y. Shao-Horn, Nat. Chem. 3 (2011) 546–550.
[20] J. Suntivich, K.J. May, H.A. Gasteiger, J.B. Goodenough, Y. Shao-Horn, Science 334 (2011) 1383–1385.
[21] A. Grimaud, K.J. May, C.E. Carlton, Y.L. Lee, M. Risch, W.T. Hong, J.G. Zhou, S.H. Yang, Nat. Commun. 4 (2013).
[22] J.J. Xu, Z.L. Wang, D. Xu, F.Z. Meng, X.B. Zhang, Energy Environ. Sci. 7 (2014) 2213–2219.
[23] J.J. Xu, D. Xu, Z.L. Wang, H.G. Wang, L.L. Zhang, X.B. Zhang, Angew. Chem. Int. Ed. 52 (2013) 3887–3890.
[24] Y.L. Zhao, L. Xu, L.Q. Mai, C.H. Han, Q.Y. An, X. Xu, X. Liu, Q.J. Zhang, Proc. Natl. Acad. Sci. USA 109 (2012) 19569–19574.
[25] D.U. Lee, H.W. Park, D. Higgins, L. Nazar, Z. Chen, J. Electrochem. Soc. 160 (2013) F910–F915.
[26] X.Y. Lu, C. Zhao, J. Mater. Chem. A 1 (2013) 12053–12059.
[27] J.B. Liu, A.C. Co, S. Paulson, V.I. Birss, Solid State Ion. 177 (2006) 377–387.
[28] S. Rousseau, S. Loridant, P. Delichere, A. Boreave, J.P. Deloume, P. Vernoux, Appl. Catal. B: Environ. 88 (2009) 438–447.
[29] H.W. Park, D.U. Lee, L.F. Nazar, Z. Chen, J. Electrochem. Soc. 160 (2013) A344–A350.
[30] Y.L. Li, J.J. Wang, X.F. Li, D.S. Geng, M.N. Banis, R.Y. Li, X.L. Sun, Electrochem. Commun. 18 (2012) 12–15.
[31] D. Wei, Y. Liu, Y. Wang, H. Zhang, L. Huang, G. Yu, Nano Lett. 9 (2009) 1752–1758.
[32] J.H. Lee, U. Paik, J.Y. Choi, K.K. Kim, S.M. Yoon, J. Lee, B.K. Kim, J.M. Kim, M.H. Park, C.W. Yang, K.H. An, Y.H. Lee, J. Phys. Chem. C 111 (2007) 2477–2483.
[33] Y.Q. Liu, L. Gao, J. Sun, Y. Wang, J. Zhang, Nanotechnology 20 (2009).
[34] D.U. Lee, B.J. Kim, Z. Chen, J. Mater. Chem. A 1 (2013) 4754–4762.
[35] R.N. Singh, B. Lal, Int. J. Hydrog. Energy 27 (2002) 45–55.

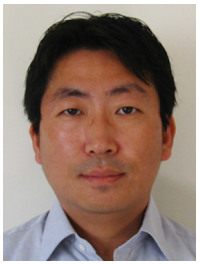

Hey Woong Park received his Bachelor's degree in Chemistry Department from Sungkyunkwan University in 2000 and Master's degree in Chemistry Department from Korea Advanced Institute of Science and Technology in 2002. Since then he joined LG Chem. in Korea as a researcher for Li-ion batteries. Currently, he is pursuing his doctoral degree developing nanostructured composites as electrochemical catalysts for rechargeable metal-air batteries under the supervision of Prof. Zhongwei Chen and Prof. Linda F. Nazar in Chemical Engineering (Nanotechnology) at the University of Waterloo.

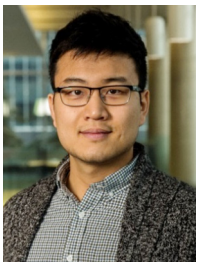

Dong Un Lee received his Bachelor's degree in Nanotechnology Engineering from the University of Waterloo in 2010. He is currently pursuing his Ph.D. in Chemical Engineering (Nanotechnology) under the supervision of Prof. Zhongwei Chen at the University of Waterloo. His research is mainly focused on the development of bi-functionally active electrocatalyst for both oxygen reduction reaction and oxygen evolution reactions for rechargeable metal-air energy conversion and storage systems.

Pouyan Zamani received his Bachelor's degree in Polymer Engineering (2007) and Master's degree in Polymer/Nanotechnology Engineering (2010) from Amirkabir University (Tehran Polytechnic). He then joined Engineering Research Institute in Tehran as a researcher. He is now pursuing his Ph.D. degree in Chemical Engineering at the University of Waterloo under Prof. Zhongwei Chen's supervision with his research focused on the development of nanostructure carbon based materials as non-precious catalysts for fuel-cell applications.

Min Ho Seo received his Bachelor's degree in Advanced Materials Science and Engineering from Sungkyunkwan University in 2005, Master's degree and Ph.D. in Materials Science from Gwangju Institute of Science and Technology in 2007 and 2012 under the supervision of Prof. Dr. Won Bae Kim. He is currently a postdoctoral fellow working with Prof. Zhongwei Chen at the University of Waterloo. His current research is mainly focused on the catalyst development based on novel support materials and non-precious catalysts for fuel-cell and metal-air battery applications through both experimental and the first principle studies (DFT).

Linda F. Nazar was born in Vancouver, Canada, and received her Ph.D. degree at the University of Toronto. After joining Exxon Corporate Research in Annandale New Jersey to take up a postdoctoral fellowship, she moved to the University of Waterloo where she is a Professor of Chemistry and Electrical Engineering, and a fellow of the Royal Society of Canada. She

holds a Senior Canada Research Chair in Solid State Energy Materials. Her solidstate electrochemistry research is focused on materials for energy storage and conversion, with research spanning Li-ion and Na-ion batteries, Li-sulfur and Li-O_2 batteries, and energy conversion materials.

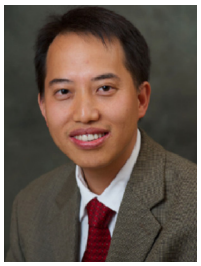

Zhongwei Chen is an Associate Professor of Chemical Engineering at the University of Waterloo. His research interests are the development of advanced electrode materials for metal-air batteries, lithium-ion batteries and fuel cells. He received his Ph.D. in Chemical and Environmental Engineering from the University of California-Riverside. Prior to joining Waterloo in 2008, he focused on advanced catalyst research at the Los Alamos National Laboratory. He has published 1 book, 5 book chapters and more than 90 peer-reviewed journal articles that have been cited over 4000 times. He is an inventor on 3 US patents and 8 provisional US patents, with two licensed to startup companies in USA.